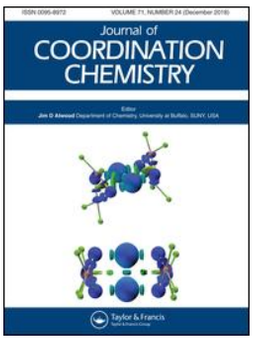

Journal of Coordination Chemistry

ISSN: 0095-8972 (Print) 1029-0389 (Online) Journal homepage: https://www.tandfonline.com/loi/gcoo20

SCMNPs@Urea/Py-$CuCl_2$: a recyclable catalyst for the synthesis of pyrano[2,3-*d*]pyrimidinone and pyrano[2,3-*d*] pyrimidine-2,4,7-trione derivatives

Jun Zhang, Hongqing Song, Ruirui Cui, Chaoyong Deng & Qahtan A. Yousif

To cite this article: Jun Zhang, Hongqing Song, Ruirui Cui, Chaoyong Deng & Qahtan A. Yousif (2020): SCMNPs@Urea/Py-$CuCl_2$: a recyclable catalyst for the synthesis of pyrano[2,3-*d*]pyrimidinone and pyrano[2,3-*d*] pyrimidine-2,4,7-trione derivatives, Journal of Coordination Chemistry, DOI: 10.1080/00958972.2020.1737681

To link to this article: https://doi.org/10.1080/00958972.2020.1737681

Published online: 23 Mar 2020.

JOURNAL OF COORDINATION CHEMISTRY
https://doi.org/10.1080/00958972.2020.1737681

Taylor & Francis
Taylor & Francis Group

SCMNPs@Urea/Py-$CuCl_2$: a recyclable catalyst for the synthesis of pyrano[2,3-*d*]pyrimidinone and pyrano[2,3-*d*]pyrimidine-2,4,7-trione derivatives

Jun Zhang[a,b,c], Hongqing Song[a,c], Ruirui Cui[a,c], Chaoyong Deng[a,c] and Qahtan A. Yousif[d]

[a]College of Big Data and Information Engineering, Guizhou University, Guiyang, Guizhou, China; [b]College of Computer and Information Engineering, Guizhou University of Commerce, Guiyang, Guizhou, China; [c]Key Laboratory of Functional Composite Materials of Guizhou Province, Guizhou University, Guiyang, Guizhou, China; [d]College of Education, Department of Chemistry, University of Al-Qadisiyah, Al Diwaniyah, Republic of Iraq

ABSTRACT

An efficient, simple, and mild strategy for the one-pot multicomponent synthesis of pyrano[2,3-*d*]pyrimidinone and pyrano[2,3-*d*]pyrimidine-2,4,7-trione derivatives is described using SCMNPs@Urea/Py-$CuCl_2$ nanoparticles as a reusable heterogeneous magnetic nanocatalyst. The catalyst was characterized using Fourier transform infrared spectroscopy (FTIR), thermogravimetric analysis (TGA), vibrating sample magnetometry (VSM), energy dispersive X-ray spectroscopy (EDX), X-ray diffraction (XRD), and scanning electron microscopy (SEM). The SCMNPs@Urea/Py-$CuCl_2$ can be easily collected from the reaction solution by magnetic decantation using a permanent magnetic field and reused in six runs without significant decrease in catalytic activity.

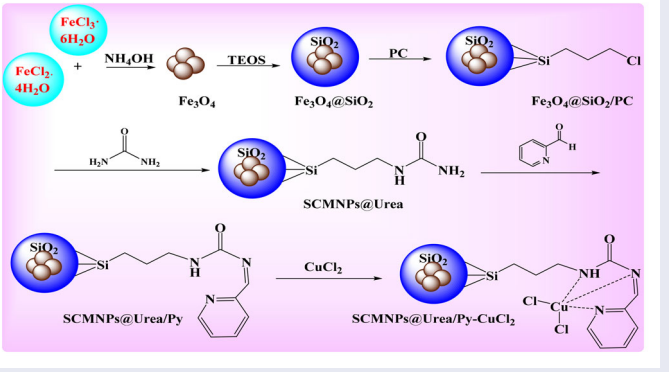

ARTICLE HISTORY
Received 10 December 2019
Accepted 10 February 2020

KEYWORDS
SCMNPs@Urea/Py-CuCl2; pyrano[2,3-d]pyrimidinone; pyrano[2,3-d]pyrimidine-2,4,7-trione; multicomponent synthesis; magnetic nanocatalyst

CONTACT Chaoyong Deng chaoyongdeng@163.com

1. Introduction

Synthesis of separable and reusable heterogeneous catalysts has received significant attention [1–6]. One strategy to achieve this purpose is the functionalization of the heterogeneous supports with homogeneous catalysts [7]. To avoid tedious work-up processes like centrifugation and filtration, the catalysts can be supported on magnetic nanoparticles as the core magnetic support and separated from the reaction media at the end of the process via an external magnetic field due to the magnetic nature of these particles. After separating, rinsing, and drying of the catalysts, they can be reused several times while keeping their primary activity. Fe_3O_4 magnetic nanoparticles (MNPs) have been widely investigated among the various utilized nanoparticles because of their technological applications [8, 9]. Naked Fe_3O_4 MNPs due to high initial chemical activity, great surface area to volume ratio, and dipole-dipole attractions between MNPs tend to oxidize and accumulate and they are susceptible to loss of their magnetic nature during the reaction period [10]. Formation of an organic (polymers, surfactants) or inorganic (silica, carbon, calcium hydroxyapatite) shell on the MNPs was introduced to overcome their drawback, which enhanced their chemical stability [11–19].

The use of barbituric acid as a 1,3-dicarbonyl compound in the synthesis of functionalized pyrimidine compounds has attracted attention because they are very important in natural material chemistry and pharmacological activities [20–22]. Synthesized derivatives of barbituric acid with alkyls and aryls have hypnotic and seductive properties while the precursor itself does not exhibit these properties [23, 24]. The pyrano fused pyrimidines like pyrimido[2,3-*d*]pyrimidinone have been investigated due to its wide-range of pharmaceutical and biological properties such as antihypertensive, antimicrobial, antitumor, antifungal, anti-inflammatory, antiallergic, antibacterial, and antimalarial [25–31]. Some of these heterocyclic compounds can be utilized in photoactive materials, cosmetics, and pigments [32, 33]. The pyrano[2,3-*d*]pyrimidine-2,4,7-triones are among other pyrano fused pyrimidines. These biologically active compounds with pyrimidinone scaffolds have attracted much attention because of their potent antitumor function in the treatment of P388 leukemia and B16 melanoma [34–36]. Also, pyrano[2,3-*d*]pyrimidine-2,4,7-triones are diverse and densely functionalized heterocyclic molecules that show antiplatelet antimicrobial, anticonvulsant, as well as antifungal activities [37–41].

2. Experimental

All the pure substances were purchased from Fluka, Merck, and Aldrich Chemical Companies. Melting points of the substrate were determined using a Büchi B-545 apparatus in open capillary tubes. FT-IR spectroscopy was performed using a Perkin Elmer spectrum BX series. TGA spectra were obtained using a Linseis SATPT 1000 thermoanalyzer. Magnetic susceptibility measurements were examined using a vibrating sample magnetometry (VSM; Lake Shore 7200 at 300 K VSM). The chemical composition was done by energy dispersive X-ray spectroscopy (EDX) on ESEM, Philips, and XL30. ICP analysis was carried out on a VISTA-PRO, CCD simultaneous ICP analyzer. Powder X-ray diffraction (XRD) was carried out on a Siemens D-500 X-ray diffractometer (Munich, Germany). Scanning electron microscopy was done with a SEM-LEO 1430VP analyzer.

2.1. Fe3O4 nano-particles preparation

To prepare Fe_3O_4 nanoparticles, a mixture of $FeCl_3{\cdot}6H_2O$ (6.68 g) and $FeCl_2{\cdot}4H_2O$ (2.55 g) was poured in 150 mL deionized water and stirred mechanically under N_2. Then, 22 mL of NH_4OH (25 wt%) was injected into the reaction solution until pH = 11. The reaction solution was stirred at 70 °C for 1 h. The resulting mixture was cooled to 25 °C and the magnetic nanoparticles were isolated by a permanent magnetic field, rinsed three times with deionized water, and dried under vacuum.

2.2. Synthesis of silica-coated magnetic nanoparticles (Fe_3O_4@SiO_2)

0.1 g of prepared Fe_3O_4 MNPs was dispersed in a solution mixture of 150 mL ethanol, 10 mL deionized water and 7 mL NH_4OH (25%) under mechanical stirring for 25 min. Then, 0.3 mL of tetraethylorthosilicate (TEOS) was added dropwise to the reaction solution under vigorous sonication for another 25 min. After continuous stirring for 7 h, the silica-coated magnetic nanoparticles were collected by magnetic decantation and then rinsed several times with water and ethanol to remove unreacted chemicals; finally, they were dried under vacuum.

2.3. Preparation of Fe_3O_4@SiO_2/PC nanoparticles

Two grams of prepared Fe_3O_4@SiO_2 nanoparticles were suspended in 50 mL of dry toluene and sonicated for 30 min in an ultrasonic bath. Then, 4 mL of 3-chloropropyltriethoxysilane (PC) was added into the reaction vessel and the reaction mixture was refluxed for 24 h under nitrogen gas. Next, the resulting solid product was isolated using a permanent magnetic field and rinsed three times with water and ethanol to remove any unreacted chemicals; finally, it was dried under vacuum.

2.4. Preparation of SCMNPs@urea

1 g of core-shell Fe_3O_4@SiO_2/PC nanoparticles and 1.2 g of KI were poured in 75 mL acetonitrile and dispersed using ultrasonication for 30 min. Next, 0.5 g of urea and 1.1 g of K_2CO_3 were added into the reaction solution and refluxed for 24 h under nitrogen. After this period, the resultant solid precipitates were collected from the solution by an external magnet and then washed several times with water/ethanol. Finally, the solid product was dried in a vacuum oven.

2.5. Preparation of SCMNPs@urea/Py

1 g of SCMNPs@Urea was dispersed in 50 mL dry ethanol under ultrasonic irradiation for 30 min. After that, 2.5 mmol of pyridine-2-carbaldehyde (Py) was added to the reaction vessel, and the mixture was stirred for 24 h under reflux conditions. Finally, the resultant solid product was isolated using an external magnet and washed thoroughly with ethanol and dried in an oven at 60 °C for 12 h.

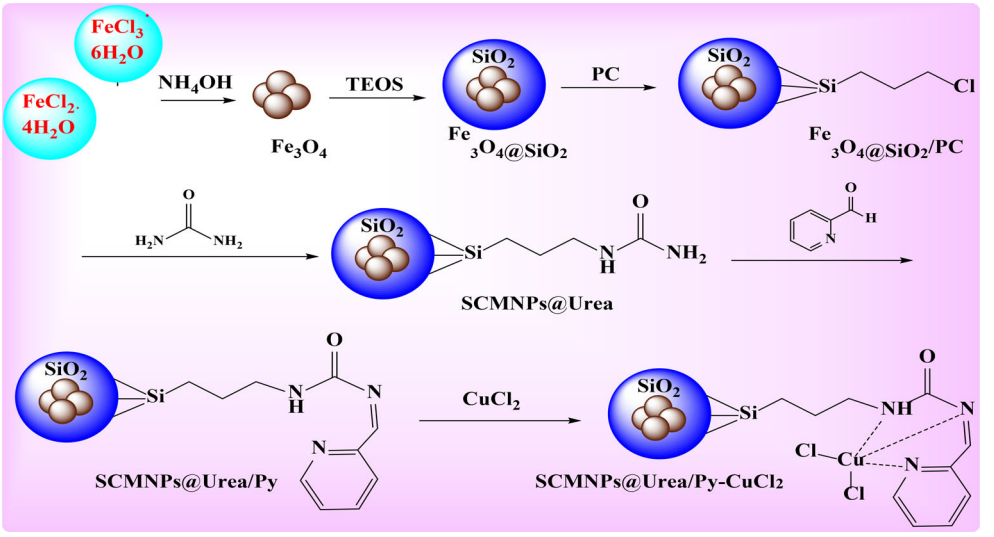

Scheme 1. The SCMNPs@Urea/Py-$CuCl_2$ synthesis.

2.6. Preparation of SCMNPs@urea/Py-$CuCl_2$

1 g of the SCMNPs@Urea/Py was dispersed in 75 mL of ethanol under ultrasonic irradiation for 30 min and 0.3 g of $CuCl_2$ was added to the reaction mixture. Afterwards, the solution was refluxed for 12 h and the solid product was collected by magnetic decantation in the presence of the external magnet, washed thoroughly with ethanol, and dried in an oven. All stages of the SCMNPs@Urea/Py-$CuCl_2$ preparation are illustrated in Scheme 1.

2.7. General process for synthesis of pyrano[2,3-d]pyrimidinone derivatives (4)

A mixture of barbituric acid (1 mmol), aldehyde (1 mmol), malononitrile (1.1 mmol), and SCMNPs@Urea/Py-$CuCl_2$ (12 mg) was refluxed in the presence of H_2O-EtOH as a suitable solvent for the appropriate time. The reaction was monitored by TLC [*n*-hexane:ethyl acetate (7:4 ratio)] analyses. At the end of the reaction, the reaction solution was cooled to room temperature and then the catalyst was removed using an external magnetic field. The remaining mixture was isolated by filtration and the achieved product was purified by re-crystallization in aqueous EtOH (25%).

2.8. General process for synthesis of pyrano[2,3-d]pyrimidine-2,4,7-trione derivatives (6)

A mixture of barbituric acid (1 mmol), aldehyde (1 mmol), Meldrum's acid (1 mmol), and SCMNPs@Urea/Py-$CuCl_2$ (15 mg) was refluxed in the presence of H_2O as a green and suitable solvent for the appropriate time. The reaction was monitored by TLC [*n*-hexane:ethyl acetate (9:5 ratio)] analyses. At the end of the reaction, the reaction solution was cooled to room temperature and then the catalyst was removed using an

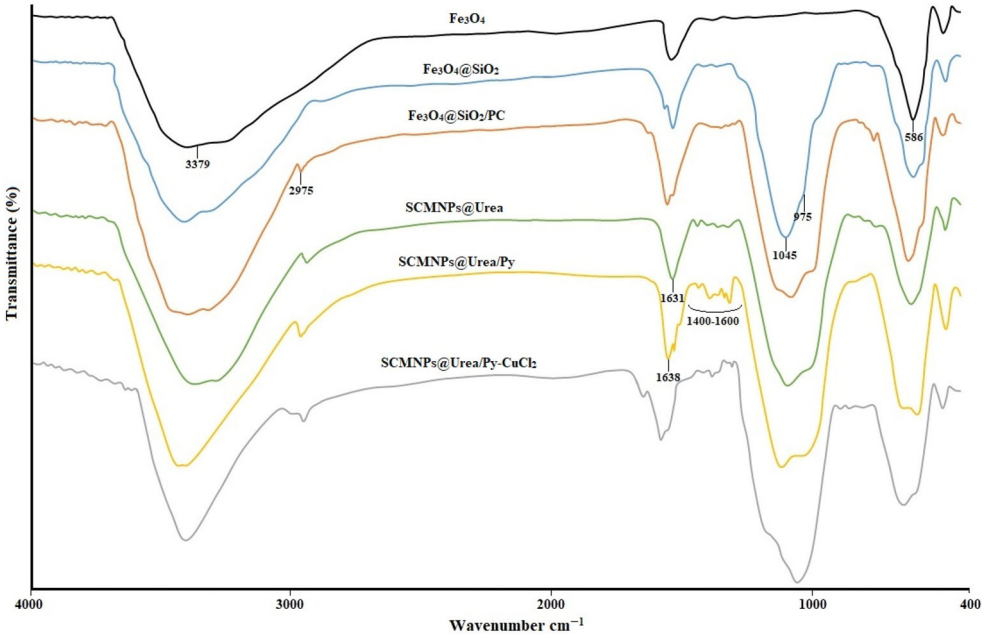

Figure 1. FTIR spectra of Fe_3O_4, Fe_3O_4@SiO_2, Fe_3O_4@SiO_2/PC, SCMNPs@Urea, SCMNPs@Urea/Py, and SCMNPs@Urea/Py-$CuCl_2$.

external magnetic field. The remaining mixture was isolated by filtration and the achieved product was purified by re-crystallization in aqueous EtOH (25%).

3. Results and discussion

3.1. FTIR analysis of SCMNPs@Urea/Py-$CuCl_2$

FT-IR spectra of Fe_3O_4, Fe_3O_4@SiO_2, Fe_3O_4@SiO_2/PC, SCMNPs@Urea, SCMNPs@Urea/Py, and SCMNPs@Urea/Py-$CuCl_2$ samples from 400 to 4000 cm^{-1} are shown in Figure 1. The bands at 586 cm^{-1} and 3379 cm^{-1} in Fe_3O_4 can be attributed to the stretching vibration of the Fe-O and O-H of the water molecule. In the FT-IR spectrum of the Fe_3O_4@SiO_2, the absorption peaks at 975 and 1045 cm^{-1} are related to the Si-O-Si and Si-OH stretches, respectively. The band at 2975 cm^{-1} of Fe_3O_4@SiO_2/PC is attributed to the C-H stretch after treating the Fe_3O_4@SiO_2 with 3-chloropropyltriethoxysilane. The FT-IR spectrum of SCMNPs@Urea illustrates the peak at 1631 cm^{-1} that is indexed to the C = O bond of the amide group. In the FTIR spectrum of SCMNPs@Urea/Py, the characteristic bands between 1400 and 1600 cm^{-1} and the absorption at 1638 cm^{-1} can be, respectively, ascribed to the C = C and C = N groups. The appearance of the same bands in the FT-IR spectrum of SCMNPs@Urea/Py-$CuCl_2$ is also confirmed.

3.2. Thermal analysis of SCMNPs@Urea/Py-$CuCl_2$

The thermal stability of Fe_3O_4, Fe_3O_4@SiO_2, Fe_3O_4@SiO_2/PC, SCMNPs@Urea, SCMNPs@Urea/Py, and SCMNPs@Urea/Py-$CuCl_2$ were also studied by thermogravimetric

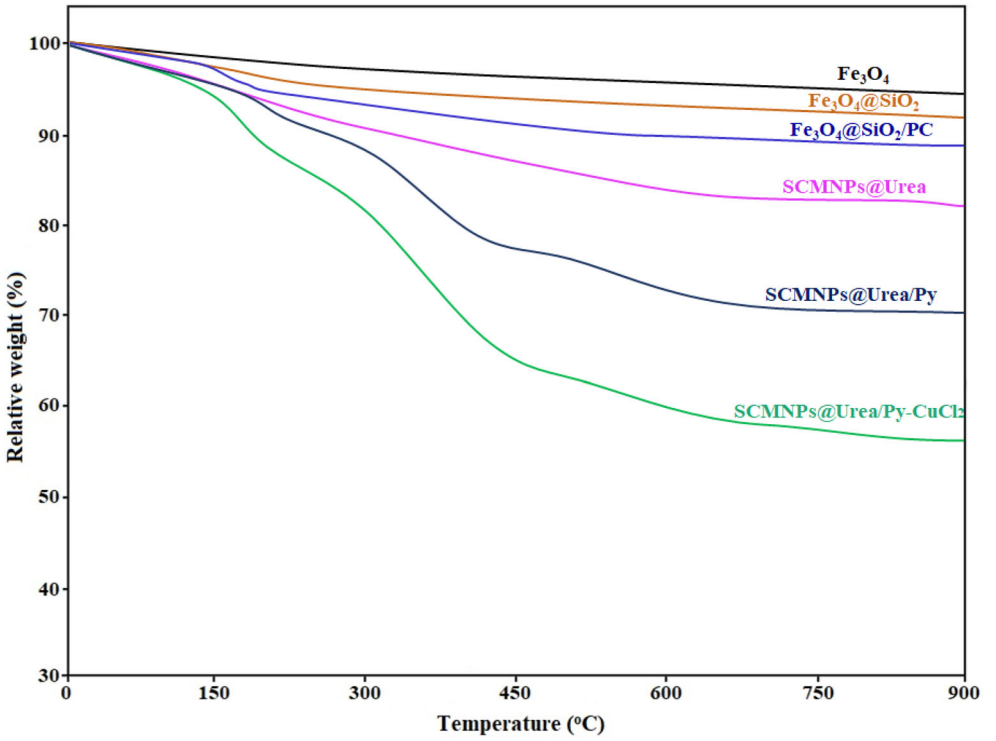

Figure 2. TGA graphs of Fe_3O_4, Fe_3O_4@SiO_2, Fe_3O_4@SiO_2/PC, SCMNPs@Urea, SCMNPs@Urea/Py, and SCMNPs@Urea/Py-$CuCl_2$.

analyzer under nitrogen at 10 °C.min^{-1} of heating rate (Figure 2). TGA data for all samples have slight weight loss below 235 °C due to evaporation of the physically adsorbed water molecules and dehydration of silica layers. Another weight loss at 430 °C was found in TGA curves of Fe_3O_4@SiO_2/PC and SCMNPs@Urea, which can be related to decomposition of attached 3-chloropropyltriethoxysilane and urea groups on the Fe_3O_4@SiO_2 surface. SCMNPs@Urea/Py and SCMNPs@Urea/Py-$CuCl_2$ have weight loss stages at 370 and 580 °C, respectively, which are associated with the decomposition of functionalized groups grafted to the Fe_3O_4 surface.

3.3. VSM analysis of SCMNPs@Urea/Py-$CuCl_2$

Magnetic features of Fe_3O_4, Fe_3O_4@SiO_2, and SCMNPs@Urea/Py-$CuCl_2$ were determined using a vibrating sample magnetometer (VSM) at ambient temperature (Figure 3). The saturation magnetization (Ms) of Fe_3O_4 and Fe_3O_4@SiO_2 were 62.56 and 50.86 emu g^{-1}, respectively, which can be related to the functionalization of the Fe_3O_4 with the silica layers. As shown, the value of the SCMNPs@Urea/Py-$CuCl_2$ saturation magnetization was 33.52 emu g^{-1}. This reduction in the value of Ms indicates formation of functional groups on the surface of the Fe_3O_4@SiO_2. The catalyst, even with this reduction in the value of Ms, can be separated from the reaction solution using an external magnetic field.

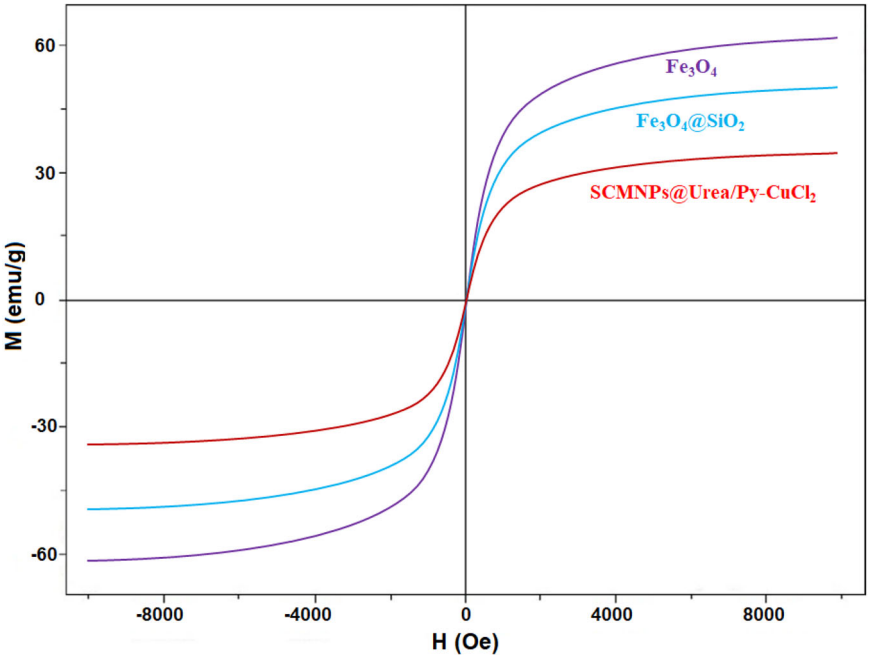

Figure 3. VSM patterns of Fe_3O_4, Fe_3O_4@SiO_2, and SCMNPs@Urea/Py-$CuCl_2$.

3.4. EDX analysis of SCMNPs@Urea/Py-$CuCl_2$

The energy dispersive X-ray (EDX) spectrum was applied to identify the elemental composition of the SCMNPs@Urea/Py-$CuCl_2$, approving the presence of all expected elements such as Fe, Si, Cu, C, N, and O (Figure 4). In addition, the ICP analysis demonstrated that 4.5% (0.7 mmol per gram) of copper was anchored on SCMNPs@Urea/Py-$CuCl_2$.

3.5. XRD analysis of SCMNPs@Urea/Py-$CuCl_2$

The XRD-diffraction patterns of Fe_3O_4 and SCMNPs@Urea/Py-$CuCl_2$ confirm the crystalline nature of these nanoparticles (Figure 5). The XRD patterns of Fe_3O_4 show several characteristic peaks at $2\theta = 32.24^\circ$ (220), 36.45° (311), 43.15° (400), 52.76° (422), 57.65° (511) and 62.84° (440), corresponding to the crystalline cubic spinel structure and they are in agreement with (JCPDS card no. 19-0629). The similar characteristic peaks were also observed for SCMNPs@Urea/Py-$CuCl_2$, indicating the stability of pure magnetic nanoparticles by surface modification with imine and a coordination complex.

3.6. SEM analysis of SCMNPs@Urea/Py-$CuCl_2$

The morphology and size of Fe_3O_4 and SCMNPs@Urea/Py-$CuCl_2$ were evaluated using scanning electron microscopy (SEM) as shown in Figure 6. The SEM images show that porous surface and spherical nanoparticles were achieved with an average diameter of 38–45 nm.

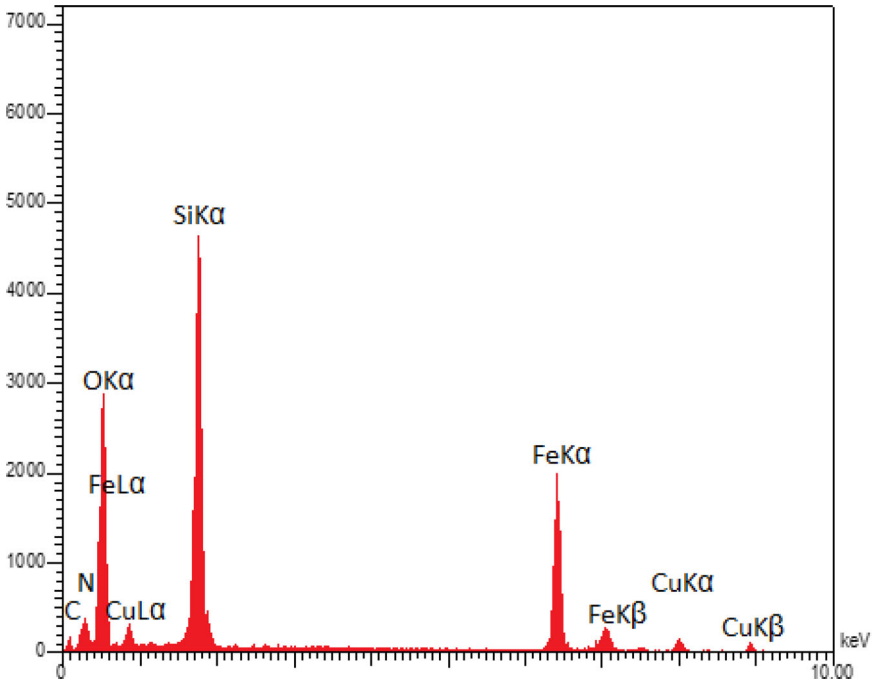

Figure 4. EDX spectrum of SCMNPs@Urea/Py-$CuCl_2$.

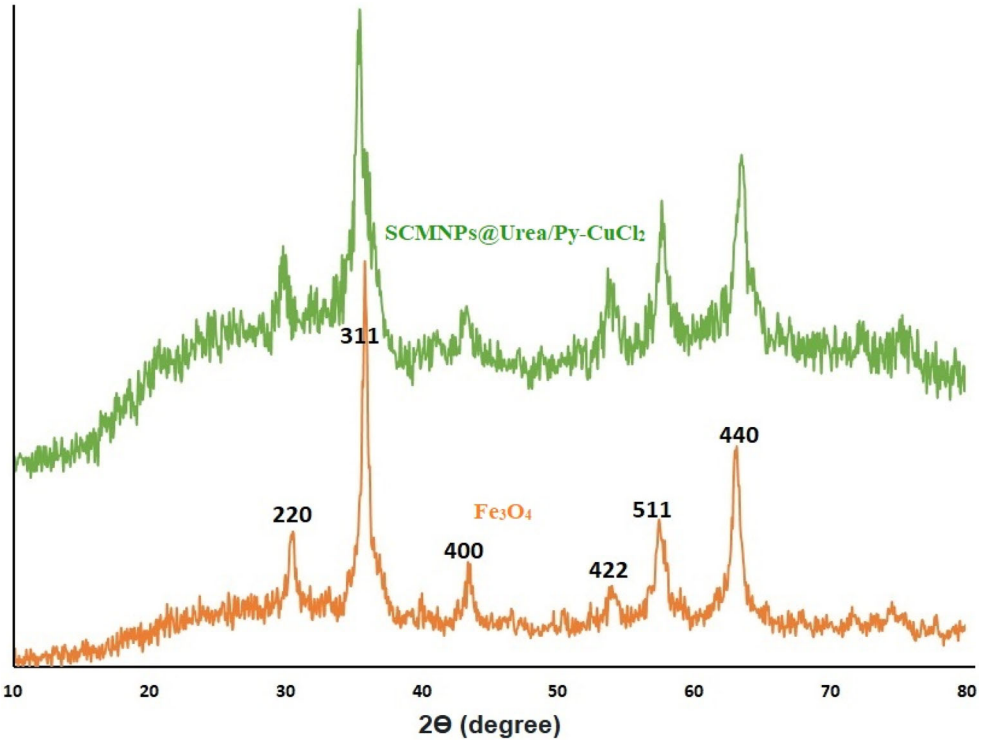

Figure 5. XRD patterns of Fe_3O_4 and SCMNPs@Urea/Py-$CuCl_2$.

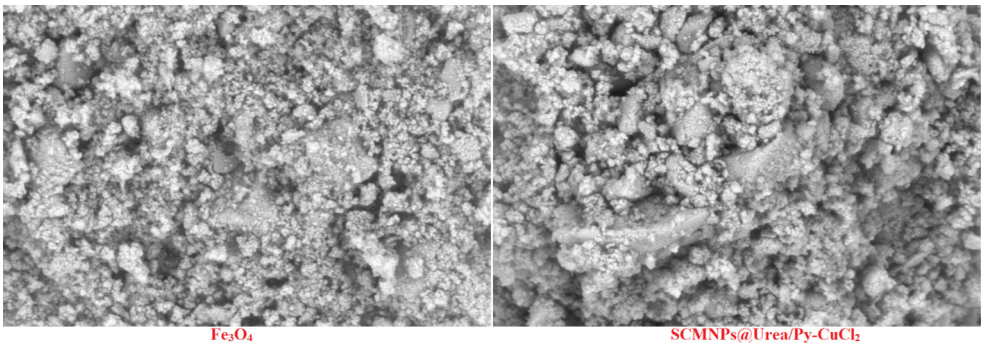

Figure 6. SEM image of Fe_3O_4 and SCMNPs@Urea/Py-$CuCl_2$.

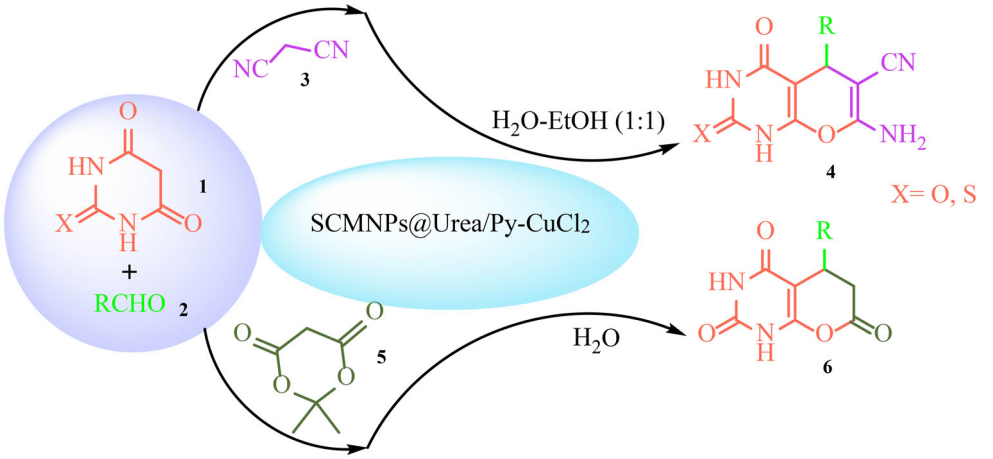

Scheme 2. Synthesis of pyrano[2,3-*d*]pyrimidinone and pyrano[2,3-*d*]pyrimidine-2,4,7-trione derivatives using SCMNPs@Urea/Py-$CuCl_2$.

Table 1. Optimization of the three-component reaction of barbituric acid (**1**), 4-chlorobenzaldehyde (**2i**), and malononitrile (**3**) under various amounts of the catalyst, temperature, and solvent[a].

Entry	Catalyst (mg)	Solvent	Temp. (°C)	Time (min)/Yield (%)
1	12	H_2O	Reflux	25/91
2	12	EtOH	Reflux	20/93
3	12	H_2O-EtOH (1:1)	Reflux	12/96
4	12	H_2O-EtOH (2:1)	Reflux	12/87
5	12	H_2O-EtOH (1:2)	Reflux	12/94
6	12	CH_3CN	Reflux	120/45
7	12	CH_2Cl_2	Reflux	120/trace
8	12	$CHCl_3$	Reflux	120/trace
9	12	–	Reflux	25/87
10	6	H_2O-EtOH (1:1)	Reflux	12/58
11	8	H_2O-EtOH (1:1)	Reflux	12/69
12	10	H_2O-EtOH (1:1)	Reflux	12/83
13	14	H_2O-EtOH (1:1)	Reflux	12/95
14	16	H_2O-EtOH (1:1)	Reflux	12/95
15	12	H_2O-EtOH (1:1)	25 °C	60/75

[a]Reaction conditions: barbituric acid (1 mmol), 4-chlorobenzaldehyde (1 mmol), malononitrile (1.1 mmol), and SCMNPs@Urea/Py-$CuCl_2$ under various conditions.

Table 2. Preparation of pyrano[2,3-d]pyrimidinone derivatives catalyzed by SCMNPs@urea/Py-$CuCl_2$[a].

Entry	Product	Aldehyde (2)	Compounds	Time (min.)	Yield(%)[b]	M.P (Obsd.) (°C)	M.P (Lit.) (°C)
1	**4a**		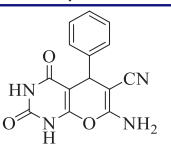	20	91	210–212	215–217 [42]
2	**4b**	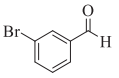	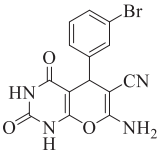	20	92	251–254	254–256 [43]
3	**4c**	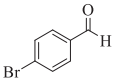	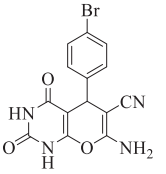	15	96	225–228	230–231 [44]
4	**4d**		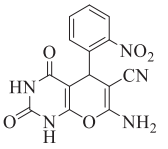	15	93	251–253	254–255 [43]
5	**4e**	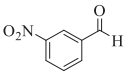	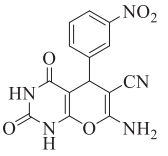	20	91	269–271	267–269 [45]
6	**4f**	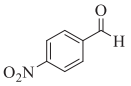	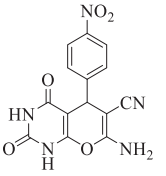	15	95	234–237	238–240 [46]
7	**4g**		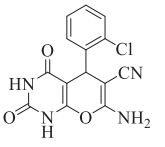	10	95	209–211	212–214 [47]
8	**4h**	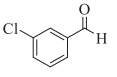	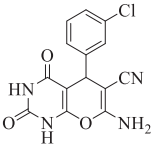	20	93	238–240	240–241 [47]

(*continued*)

Table 2. Continued.

Entry	Product	Aldehyde (2)	Compounds	Time (min.)	Yield(%)[b]	M.P (Obsd.) (°C)	M.P (Lit.) (°C)
9	**4i**	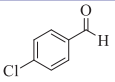	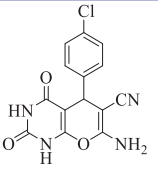	12	96	237–239	242–243 [42]
10	**4j**	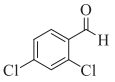	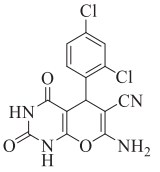	12	94	231–234	233–235 [48]
11	**4k**	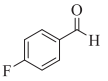	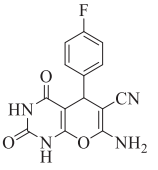	15	92	265–268	268–270 [46]
12	**4l**	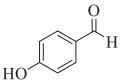	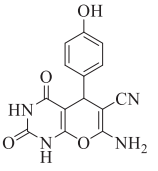	25	91	295–298	>300 [43]
13	**4m**	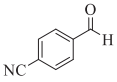	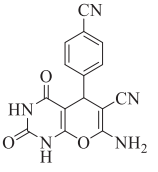	15	96	248–251	254–256 [48]
14	**4n**		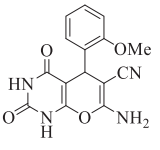	20	90	238–240	233–235 [43]
15	**4o**	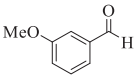	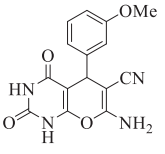	25	88	237–239	234–236 [43]
16	**4p**	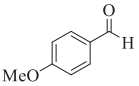	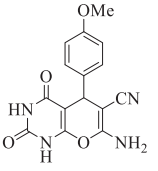	18	92	272–274	266–270 [49]

(*continued*)

Table 2. Continued.

Entry	Product	Aldehyde (2)	Compounds	Time (min.)	Yield(%)[b]	M.P (Obsd.) (°C)	M.P (Lit.) (°C)
17	**4q**	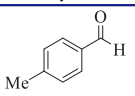	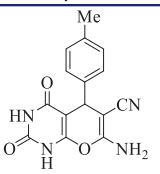	15	91	229–231	228–230 [50]
18	**4r**		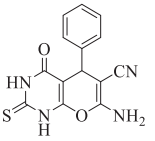	15	87	222–224	224–225 [42]
19	**4s**		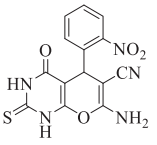	20	90	239–241	242–246 [49]
20	**4t**	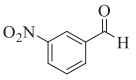	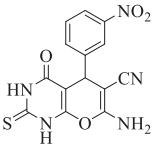	20	89	230–232	234–235 [49]
21	**4u**	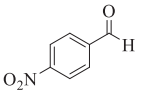	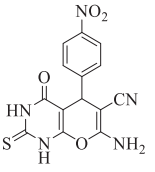	15	92	237–239	235–236 [44]
22	**4v**	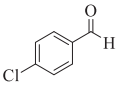	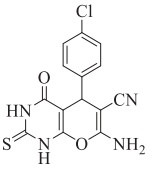	18	90	>300	>300 [42]
23	**4w**	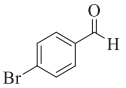	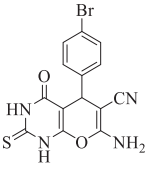	15	94	256–258	236(dec.) [44]

[a]Reaction conditions: barbituric acid (1 mmol), aldehyde (1 mmol), malononitrile (1.1 mmol), and 12 mg of the SCMNPs@Urea/Py-$CuCl_2$.
[b]The yields refer to the isolated product.

In this study, we investigate the effect of this recyclable magnetic catalyst on the synthesis of pyrano[2,3-*d*]pyrimidinone and pyrano[2,3-*d*]pyrimidine-2,4,7-trione derivatives (Scheme 2).

To optimize the conditions of the reaction for preparation of the 7-amino-5-(4-chlorophenyl)−2,4-dioxo-1,3,4,5-tetrahydro-2*H*-pyrano[2,3-*d*]pyrimidine-6-carbonitrile,

Table 3. Optimization of the three-component reaction of barbituric acid (**1**), 4-chlorobenzaldehyde (**2h**), and meldrum's acid (**5**), under various amounts of the catalyst, temperature, and solvent[a].

Entry	Catalyst (mg)	Solvent	Temp. (°C)	Time (min)/Yield (%)
1	15	H_2O	Reflux	30/95
2	15	EtOH	Reflux	40/85
3	15	H_2O-EtOH (1:1)	Reflux	30/91
4	15	Toluene	Reflux	120/42
5	15	CH_3OH	Reflux	60/74
6	15	CH_3CN	Reflux	120/62
7	15	CH_2Cl_2	Reflux	120/60
8	15	$CHCl_3$	Reflux	120/56
9	15	–	Reflux	30/89
10	8	H_2O	Reflux	50/62
11	10	H_2O	Reflux	45/69
12	12	H_2O	Reflux	36/87
13	17	H_2O	Reflux	30/94
14	20	H_2O	Reflux	30/92
15	12	H_2O	25 °C	55/73

[a]Reaction conditions: barbituric acid (1 mmol), 4-chlorobenzaldehyde (1 mmol), Meldrum's acid (1 mmol), and SCMNPs@Urea/Py-$CuCl_2$ under various conditions.

we commenced the study by treating a mixture of barbituric acid **1**, 4-chlorobenzaldehyde **2i**, and malononitrile **3** under various temperatures, solvents, and amounts of the catalyst (Table 1). To corroborate the interference of solvents during this reaction, we performed the model reaction in the presence of H_2O, EtOH, H_2O-EtOH, CH_3CN, CH_2Cl_2, $CHCl_3$, and solvent-free conditions (Table 1, entries 1–9). The best result of the reaction was achieved in the presence of H_2O-EtOH as a suitable solvent after 12 min of starting the reaction (Table 1, entry 3). To continue optimization of the reaction conditions, we tested the effect of catalyst concentration by carrying out the model reaction at concentrations ranging from 6 to 16 mg (Table 1, entries 3 and 10–14). As shown, 12 mg was the optimum concentration of the catalyst in terms of product yield and reaction time (Table 1, entry 3). Performing the model reaction in concentrations above or below 12 mg did not produce the desired results compared to the optimized value (Table 1, entries 10–14). Note that carrying out the reaction at room temperature led to formation of the target product **4i** in moderate yield and long reaction time (Table 1, entry 15).

With a set of optimized reaction conditions at hand, we generalized the scope of this transformation process for the preparation of pyrano[2,3-*d*]pyrimidinone derivatives. Various aryl aldehydes with both electron-withdrawing and electron-donating substituents were efficiently reacted with malononitrile and barbituric acid/(thio) barbituric acid, which produced high-to-excellent yields of target products (**4a-w**) in less reaction times. The results are summarized in Table 2.

For the optimization of the desired organic transformation conditions, the reaction of barbituric acid **1**, 4-cholorobenzaldehyde **2 h**, and Meldrum's acid **5** is selected as a model reaction under various temperatures, solvents and amounts of the catalyst (Table 3). Initially, the model reaction was performed in the presence of various solvents such as H_2O, EtOH, H_2O-EtOH, toluene, CH_3OH, CH_3CN, CH_2Cl_2, $CHCl_3$ and solvent-free conditions (Table 3, entries 1–9). When the desired reaction was used in H_2O as the solvent, the time and yield of the reaction became shorter and higher, respectively (Table 3, entry 1). After the selection of H_2O as the best solvent, various amounts

Table 4. Preparation of pyrano[2,3-d]pyrimidine-2,4,7-trione derivatives catalyzed by SCMNPs@urea/Py-$CuCl_2$[a].

Entry	Product	Aldehyde (2)	Product	Time (min.)	Yield(%)[b]	M.P (Obsd.) (°C)	M.P (Lit/) (°C)
1	**6a**		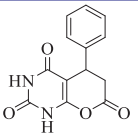	45	94	245–248	254–256 [51]
2	**6b**	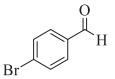	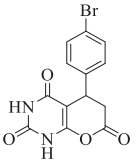	40	93	265–268	273–275 [51]
2	**6b**	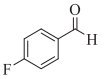	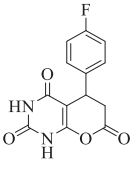	40	95	270–272	264–266 [52]
3	**6c**		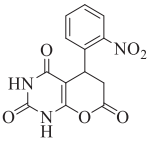	35	95	218–221	216–218 [52]
4	**6d**	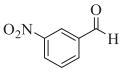	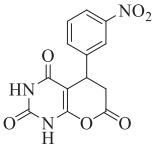	40	92	270–272	273 [53]
5	**6e**	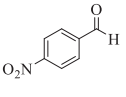	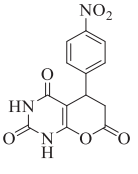	35	94	243–246	250–252 [52]
6	**6f**		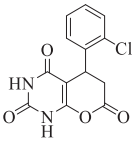	30	94	240–242	242–244 [52]
7	**6g**	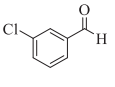	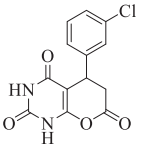	40	91	262–264	268–270 [51]

(*continued*)

Table 4. Continued.

Entry	Product	Aldehyde (2)	Product	Time (min.)	Yield(%)[b]	M.P (Obsd.) (°C)	M.P (Lit/) (°C)
8	**6h**	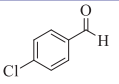	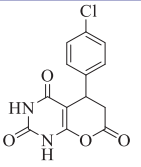	30	95	287–299	284–286 [52]
9	**6i**		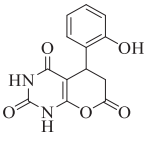	45	90	293–295	290–292 [52]
10	**6j**	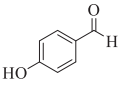	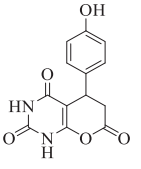	45	92	297–299	>300 [51]
11	**6k**	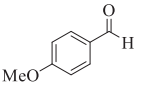	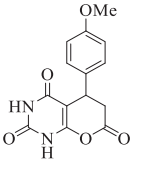	40	93	282–284	291–293 [51]
12	**6l**	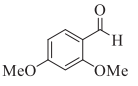	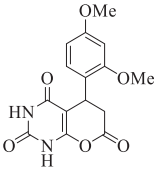	40	92	232–234	235–237 [53]
13	**6m**	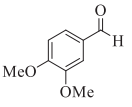	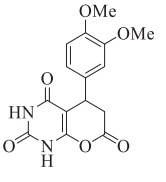	45	93	271–274	277 [53]
14	**6n**	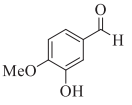	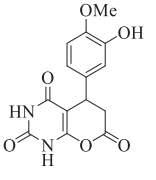	35	95	291–294	290–291 [51]
15	**6o**	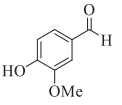	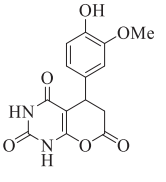	35	94	281–233	280–282 [51]

(*continued*)

Table 4. Continued.

Entry	Product	Aldehyde (2)	Product	Time (min.)	Yield(%)[b]	M.P (Obsd.) (°C)	M.P (Lit/) (°C)
16	**6p**	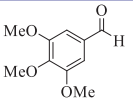	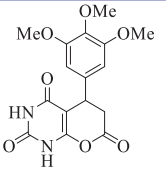	35	92	263–265	268–270 [51]
17	**6q**	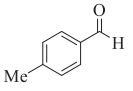	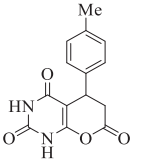	30	93	265–268	260–261 [51]
18	**6r**	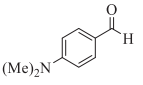	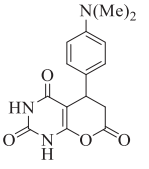	40	90	289–291	280–282 [51]

[a]Reaction conditions: barbituric acid (1 mmol), aldehyde (1 mmol), Meldrum's acid (1 mmol), and 15 mg of the SCMNPs@Urea/Py-$CuCl_2$.
[b]The yields refer to the isolated product.

of the catalyst ranging from 8 to 20 mg were selected to generate the requested products (Table 3, entries 1 and 10–14). When the reaction was performed with 15 mg of the catalyst, the reaction produced the highest yield of the product with less reaction time (Table 3, entry 1). Carrying out the reaction in high or low concentrations of the catalyst relative to the optimized value did not lead to highest yields of the product (Table 3, entries 10–14). At room temperature, when the reaction was done in H_2O, moderate percentage of the desired product was obtained in longer reaction time (Table 3, entry 15).

According to the best optimal condition achieved, several pyrano[2,3-*d*]pyrimidine-2,4,7-trione derivatives were prepared and the outcomes are listed in Table 4. To study the catalyst efficiency to determine the scope of the present system, various pyrimidines (**6a–r**) were synthesized by the one-pot condensation reaction of a barbituric acid, wide range of aromatic aldehydes with both electron-withdrawing and electron-donating substituents, and Meldrum's acid at high-to-excellent yields and in shorter reaction times. The results are shown in Table 4.

A probable mechanism for the synthesis of pyrano[2,3-*d*]pyrimidinone and pyrano[2,3-*d*]pyrimidine-2,4,7-trione derivatives catalyzed by SCMNPs@Urea/Py-$CuCl_2$ is presented in Scheme 3. The first step may be initiated with the Knoevenagel condensation of malononitrile **3**/Meldrum's acid **5** to activated carbonyl group of aldehyde **2** by the catalyst, resulting in intermediates **7** and **8**. These intermediates may further tolerate Michael addition with barbituric acid **1** and generate polar transition states **9** and **10**. These unstable intermediates undergo an intramolecular cyclization, dehydration and aromatization to afford desired products **4** and **6**.

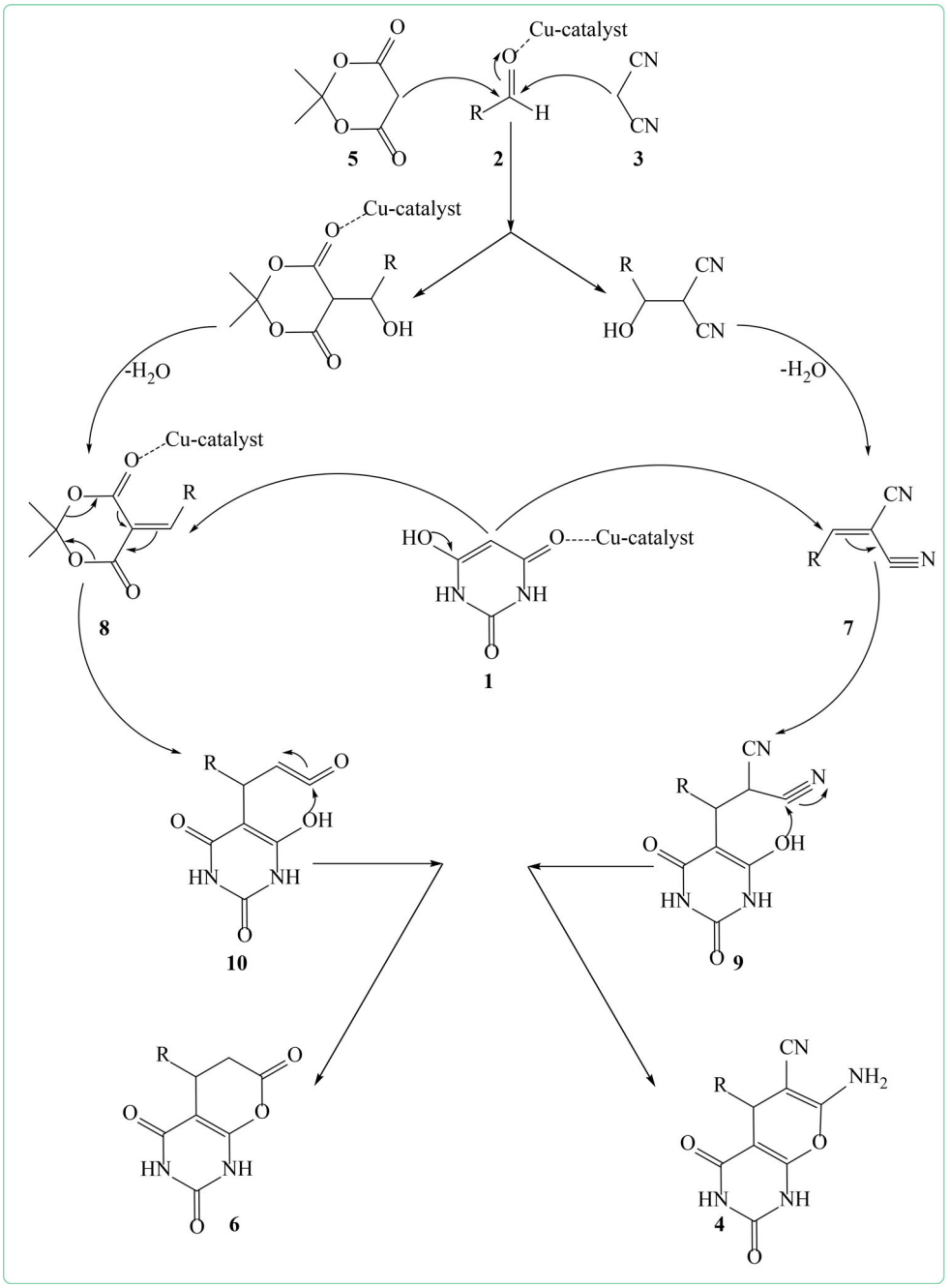

Scheme 3. A plausible mechanism for the one-pot, three-component reaction of barbituric acid **1**, aldehyde **2**, and malononitrile **3**/Meldrum's acid **5** catalyzed by SCMNPs@Urea/Py-$CuCl_2$.

Recyclability of the synthesized catalyst was investigated for preparation of 7-amino-5-(4-chlorophenyl)−2,4-dioxo-1,3,4,5-tetrahydro-2*H*-pyrano[2,3-*d*]pyrimidine-6-carbonitrile **4i** (a) and 5-(4-chlorophenyl)−5,6-dihydro-2*H*-pyrano[2,3-*d*]pyrimidine-2,4,7(1*H*,3*H*)-trione **6h** (b) in the presence of SCMNPs@Urea/Py-$CuCl_2$. Upon completion of the reaction,

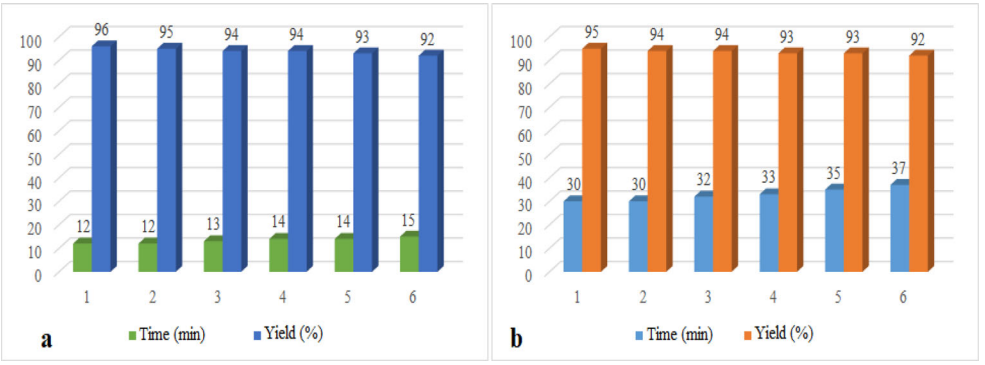

Figure 7. The recycling of SCMNPs@Urea/Py-$CuCl_2$ in the synthesis of 7-amino-5-(4-chlorophenyl)-2,4-dioxo-1,3,4,5-tetrahydro-2*H*-pyrano[2,3-*d*]pyrimidine-6-carbonitrile **4i** (a) and 5-(4-chlorophenyl)-5,6-dihydro-2*H*-pyrano[2,3-*d*]pyrimidine-2,4,7(1*H*,3*H*)-trione **6h** (b).

Table 5. Comparison of the results of the production of products **4i** (entries 1–5) and **6h** (entries 6–10).

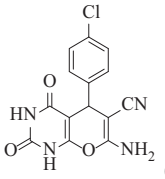

(4i)

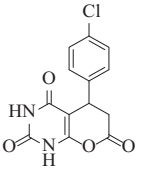

(6h)

Entry	Catalyst and conditions	Reaction time (min.)	Yield (%)[b]	Ref.
1	l-Proline/H_2O:EtOH/25 °C	45	73	[54]
2	SBA-Pr-SO_3H/Solvent-free/140 °C	15	90	[55]
3	TBAB/H_2O/Reflux	35	80	[56]
4	DABCO/H_2O:EtOH/25 °C	120	92	[57]
5	SCMNPs@Urea/Py-$CuCl_2$/H_2O:EtOH/Reflux	12	96	This work
6	CAN/H_2O/Ultrasound	40	83	[52]
7	K_2CO_3/MW	45	95	[53]
8	β-Cyclodextrin/H_2O/Ultrasound	60	88	[51]
9	Electrolys-NaBr/EtOH	240	97	[58]
10	SCMNPs@Urea/Py-$CuCl_2$/H_2O/Reflux	30	95	This work

the catalyst was extracted from the reaction mixture by permanent magnetic field, rinsed with hot ethanol and reused for the next run. The recycled catalyst was reused at least in six runs to catalyze the reaction without any notable decreases in the product yield (Figure 7). To illustrate the efficiency and applicability of SCMNPs@Urea/Py-$CuCl_2$ compared to those of other reported homogeneous and heterogeneous catalysts, we assessed the outcomes achieved for the preparation of 7-amino-5-(4-chlorophenyl)−2,4-dioxo-1,3,4,5-tetrahydro-2*H*-pyrano[2,3-*d*]pyrimidine-6-carbonitrile **4i** (a) and 5-(4-chlorophenyl)−5,6-dihydro-2*H*-pyrano[2,3-*d*]pyrimidine-2,4,7(1*H*,3*H*)-trione **6 h** (b) under various conditions. The outcomes in Table 5 illustrate that our method required lower amounts of the catalyst and provided appropriate reaction times and highest yields of the product compared to previously reported catalysts.

4. Conclusion

A new and reusable heterogeneous magnetic nanocatalyst, SCMNPs@Urea/Py-$CuCl_2$, was prepared and characterized by Fourier transform infrared spectroscopy (FTIR), thermogravimetric analysis (TGA), vibrating sample magnetometry (VSM), energy dispersive X-ray spectroscopy (EDX), X-ray diffraction (XRD), and scanning electron microscopy (SEM). SCMNPs@Urea/Py-$CuCl_2$ was proven to be an effective nanocatalyst for the synthesis of pyrano[2,3-*d*]pyrimidinone and pyrano[2,3-*d*]pyrimidine-2,4,7-trione derivatives via two one-pot, three-component reactions under solvent-free conditions. This strategy offers several key characteristics such as omitting toxic solvents, high percentages of the products, less reaction times, very simple work-up, and magnetic separation by an external magnetic field. This catalyst exhibited suitable recyclability with no considerable decrease in the catalytic behavior even after six runs.

Acknowledgement

This work was supported by National Natural Science Fund of China (No. 51762010), Guizhou Provincial High-level innovative talents (2015-4006).

Disclosure statement

No potential conflict of interest was reported by the authors.

Funding

This work was supported by National Natural Science Fund of China (No. 51762010), Guizhou Provincial High-level innovative talents (2015-4006).

References

[1] G. Schmid. *Nanoparticles: From Theory to Application*, 1st Edn, pp. 199–220, Wiley-VCH, Weinheim (2004).
[2] A.-H. Lu, E.L. Salabas, F. Schüth. *Angew. Chem. Int. Ed.*, **46**, 1222 (2007).
[3] Y. Liu, J. Zhang, X. Zhang, B. Li, X. Wang, H. Cao, D. Wei, Z. Zhou, A.K. Cheetham. *J. Mater. Chem. A*, **4**, 4280 (2016).
[4] S. Duan, G. Han, Y. Su, X. Zhang, Y. Liu, X. Wu, B. Li. *Langmuir*, **32**, 6272 (2016).
[5] C. Xing, Y. Liu, Y. Su, Y. Chen, S. Hao, X. Wu, X. Wang, H. Cao, B. Li. *ACS Appl. Mater. Interfaces*, **8**, 15430 (2016).
[6] G.A. Somorjai, J.Y. Park. *Angew. Chem. Int. Ed.*, **47**, 9212 (2008).
[7] K. Niknam, D. Saberi. *Tetrahedron Lett.*, **50**, 5210 (2009).
[8] M. Hosseini-Sarvari, A. Khanivar, F. Moeini. *J. Iran. Chem. Soc.*, **13**, 45 (2016).
[9] L. Shiri, A. Ghorbani-Choghamarani, M. Kazemi. *Aust. J. Chem.*, **69**, 585 (2016).
[10] W. Wu, Q. He, C. Jiang. *Nanoscale Res. Lett.*, **3**, 397 (2008).
[11] W. Teunissen, A.A. Bol, J.W. Geus. *Catal. Today*, **48**, 329 (1999).
[12] T.J. Yoon, W. Lee, Y.S. Oh, J.-K. Lee. *New J. Chem*, **27**, 227 (2003).
[13] H. Yoon, S. Ko, J. Jang. *Chem. Commun.*, **14,** 1468 (2007).

[14] H.H. Yang, S.Q. Zhang, X.L. Chen, Z.X. Zhuang, J.G. Xu, X.R. Wang. *Anal. Chem.*, **76**, 1316 (2004).
[15] P.D. Stevens, G. Li, J. Fan, M. Yen, Y. Gao. *Chem. Commun.*, **35**, 4435 (2005).
[16] D. Lee, J. Lee, H. Lee, S. Jin, T. Hyeon, B.M. Kim. *Adv. Synth. Catal.*, **348**, 41 (2006).
[17] C.O. Dalaigh, S.A. Corr, Y. Gun'ko, S.J. Connon. *Angew. Chem. Int. Ed.*, **46**, 4329 (2007).
[18] Y. Zhang, Z. Li, W. Sun, C. Xia. *Catal. Commun.*, **10**, 237 (2008).
[19] K. Liu, W.Z. Wei, J.X. Zeng, X.Y. Liu, Y.P. Gao. *Anal. Bioanal. Chem.*, **385**, 724 (2006).
[20] A. Shaabani, A. Maleki. *Chem. Pap.*, **61**, 333 (2007).
[21] A. Shaabani, M. Seyyedhamzeh, A. Maleki, F. Rezazadeh, M. Behnam. *J. Comb. Chem.*, **11**, 375 (2009).
[22] A. Maleki, J. Rahimi, O.M. Demchuk, A.Z. Wilczewska, R. Jasiński. *Ultrason. Sonochem.*, **43**, 262 (2018).
[23] K. Tanka, X. Cheng, F. Yoneda. *Tetrahedron*, **44**, 3241 (1988).
[24] B.B. Sokmen, S. Ugras, H.Y. Sarikaya, H.I. Ugras, R. Yanardag. *Appl. Biochem. Biotechnol.*, **171**, 2030 (2013).
[25] I.O. Donkor, C.L. Klein, L. Liang, N. Zhu, E. Bradley, A.M. Clark. *J. Pharm. Sci.*, **84**, 661 (1995).
[26] J. Quiroga, C. Cisneros, B. Insuasty, R. Abonia, S. Cruz, M. Nogueras, J.M. de la Torre, M. Sortino, S. Zacchino. *J. Heterocycl. Chem.*, **43**, 299 (2006).
[27] A.B. Deyanov, R.K. Niyazov, F.Y. Nazmetdinov, B.Y. Syropyatov, V.E. Kolla, M.E. Konshin. *Pharm. Chem. J.*, **25**, 248 (1991).
[28] G. Grossi, M. Di Braccio, G. Roma, V. Ballabeni, M. Tognolini, E. Barocelli. *Eur. J. Med. Chem.*, **40**, 155 (2005).
[29] B. Insuasty, D. Becerra, J. Quiroga, R. Abonia, M. Nogueras, J. Cobo. *Eur. J. Med. Chem.*, **60**, 1 (2013).
[30] M.M. Ghorab, A.Y. Hassan. *Phosphorus, Sulfur, Silicon Relat. Elem.*, **141**, 251 (1998).
[31] J. Davoll, J. Clarke, E.F. Elslager. *J. Med. Chem.*, **15**, 837 (1972).
[32] D. Armesto, W.M. Horspool, N. Martin, A. Ramos, C. Seoane. *J. Org. Chem.*, **54**, 3069 (1989).
[33] E.A.A. Hafez, M.H. Elnagdi, A.G.A. Elagamey, M.A.A. Ei-Taweel. *Heterocycles*, **26**, 903 (1987).
[34] K. Sharma, S. Jayakumar, M.S. Hundal, M.P. Mahajan. *J. Chem. Soc. Perkin Trans. 1*, **1**, 774 (2002).
[35] S. Sasaki, N. Cho, Y. Nara, M. Harada, S. Endo, N. Suzuki, S. Furuya, M. Fujino. *J. Med. Chem.*, **46**, 113 (2003).
[36] L.H. Li, T.L. Wallace, K.A. Richard, D.E. Tracey. *Cancer Res.*, **45**, 532(1985).
[37] N.R. Kamdar, D.D. Haveliwala, P.T. Mistry, S.K. Patel. *Eur. J. Med. Chem.*, **45**, 5056 (2010).
[38] M.E. Abdel Fattah, A.H. Atta, I.I. Abdel Gawad, S.M. Mina. *Orient. J. Chem.*, **20**, 257 (2004).
[39] O. Bruno, C. Brullo, A. Ranise, S. Schenone, F. Bondavalli, E. Barocelli, V. Ballabeni, M. Chiavarini, M. Tognolini, M. Impicciatore. *Bioorg. Med. Chem. Lett*, **11**, 1397 (2001).
[40] V.K. Akluwalia, M. Bala. *Indian J. Chem. B*, **35B**, 742 (1996).
[41] H. Shamroukh, M.E.A. Zaki, E.M.H. Morsy, F.M. Abdel-Motti, F.M.E. Abdel-Megeid. *Arch. Pharm.*, **340**, 236 (2007).
[42] B. Sabour, M.H. Peyrovi, M. Hajimohammadi. *Res. Chem. Intermed.*, **41**, 1343 (2015).
[43] N. Daneshvar, M. Nasiri, M. Shirzad, M.S.N. Langarudi, F. Shirini, H. Tajik. *New J. Chem.*, **42**, 9744 (2018).
[44] S. Balalaie, S. Abdolmohammadi, H.R. Bijanzadeh, A.M. Amani. *Mol. Divers.*, **12**, 85 (2008).
[45] O. Goli-Jolodar, F. Shirini, M. Seddighi. *J. Iran. Chem. Soc.*, **13**, 457 (2016).
[46] J. Albadi, A. Mansournezhad, T. Sadeghi. *Res. Chem. Intermed.*, **41**, 8317 (2015).
[47] B. Sadeghi, M. Bouslik, M.R. Shishehbore. *J. Iran. Chem. Soc.*, **12**, 1801 (2015).
[48] O. Goli-Jolodar, F. Shirini. *J. Iran. Chem. Soc.*, **14**, 1235 (2017).
[49] N. Seyyedi, F. Shirini, M.S.N. Langarudi. *RSC Adv.*, **6**, 44630 (2016).
[50] N. Daneshvar, F. Shirini, M.S.N. Langarudi, R. Karimi-Chayjani. *Bioorg. Chem.*, **77**, 68 (2018).
[51] M.R. Bhosle, P. Andil, D. Wahul, G.M. Bondle, A. Sarkate, S.V. Tiwari. *J. Iran. Chem. Soc.*, **16**, 1553 (2019).
[52] A. Dandia, S.L. Gupta, S. Bhaskaran. *Eur. Chem. Bull.*, **2**, 836 (2013).

[53] S.H.S. Azzam, M.A. Pasha. *Tetrahedron Lett.*, **53**, 7056 (2012).
[54] M. Bararjanian, S. Balalaie, B. Movassag, A.M. Amani. *JICS*, **6**, 436 (2009).
[55] G.M. Ziarani, S. Faramarzi, S. Asadi, V.A. Badiei, R. Bazl, M. Amanlou. *DARU. J. Pharm. Sci.*, **21**, 3(2013).
[56] A. Mobinikhaledi, M.A.B. Fard. *Acta Chim. Slov.*, **57**, 931 (2010).
[57] J. Azizian, A.L. Shameli, S. Balalaie, M. Ghanbari, S. Zomorodbakhsh, M. Entezari, S. Bagheri, G. Fakhrpour. *Orient. J. Chem.*, **28**, 327 (2012).
[58] H. Veisi, A. Maleki, Z. Omrani, S. Lotfi. *RSC Adv.*, **4**, 55313 (2014).